MATERIALE PLASTICE
https://revmaterialeplastice.ro
https://doi.org/10.37358/Mat.Plast.1964

Poly (L-lactic acid) Modified by *N, N'-bis*(Stearic acid)-1,4-Dicarboxybenzene Dihydrazide: Studies of Crystallization, Melting Behavior and Thermal Decomposition

HAO HUANG, SHUANG-QING LIU, CHENG-PEI LI, SHI-TIANLE LUO, LI-SHA ZHAO, YAN-HUA CAI*
Chongqing Key Laboratory of Environmental Materials & Remediation Technologies, College of Chemistry and Environmental Engineering, Chongqing University of Arts and Sciences, Chongqing-402160, P.R. China

Abstract: *In this study, a new organic nucleating agent N, N'-bis(stearic acid)-1,4-dicarboxybenzene dihydrazide (PASH) to improve crystallization behavior of poly(L-lactic acid) (PLLA) along with the effect of PASH on melting behavior, thermal stability of PASH-nucleated PLLA was holistically reported. The melt-crystallization process illustrated that PASH as an effective heterogeneous nucleating agent could boost PLLA's crystallization rate, but increasing PASH concentration and cooling rate conversely inhibited melt-crystallization process of PLLA in this study. With respect to melt-crystallization process, a larger amount of PASH leaded to a shift of cold-crystallization peak to lower temperature level. Isothermal crystallization revealed, in comparison to pure PLLA, that the half time of overall crystallization of PLLA/PASH was significantly decreased with PLLA containing 3 wt% PASH having the minimum $t_{1/2}$= 67.3 s at 105ºC. The different melting behaviors of PLLA/PASH under different conditions were attributed to the nucleating effect of PASH within PLLA. In particular, the melting behavior at a heating rate of 10°C/min after isothermal crystallization depended primarily on the crystallization temperature. Whereas, the impact of crystallization time on melting behavior was negligible. Nonetheless, the melting behavior was influenced by the heating rate after non-isothermal crystallization. The thermal stability of PLLA was detrimental with the addition of PASH owing to a typical drop in onset thermal decomposition temperature.*

Keywords: *PLLA, organic nucleating agent, Non-isothermal crystallization, melting process, thermal stability*

1.Introduction

A large-scale usage of petroleum-based plastics has led to critical environmental pollution, which gradually hinder the development of economy and society to a great extent. Thus, the utilization of environmentally-friendly plastics as an alternative to petroleum-based counterparts is very important to maintain the sustainable ecological development. Poly(L-lactic acid) (PLLA), derived from renewable resources such as sugarcanes, corn and potatoes [1], is one of the most popular alternative to white pollutable plastic because of its excellent biodegradability, biocompatibility, non-toxicity, compo-stability and easy processability [2, 3]. Up till now, numerous applications based on PLLA emerge commercially in food packaging [4, 5], biomedicine [6], 3D printing [7, 8], textile [9, 10], etc. Lai *et al* [11] employed an electrospinning technology to prepare PLLA/Fe_3O_4 nanofibers, and the histological results showed that the artificial bony defects grafted with PLLA/Fe_3O_4 nanofibers exhibited a higher bone healing activity when compared to those grafted with pure PLLA. Moreover, associated CT images revealed that bony defects grafted with PLLA/Fe_3O_4 nanofibers demonstrated an increases in bone volume with increasing Fe_3O_4 content, suggesting that PLLA/Fe_3O_4 nanofibers could be utilized to be a useful biomaterial for bone tissue engineering applications.

Unfortunately PLLA suffers from inherently slow crystallization rate, low crystallinity and poor heat resistance. Such drawbacks inevitably undermine its competitiveness as opposed to petroleum-based

email: caiyh651@aliyun.com

thermoplastics like polypropylene (PP) and polyethylene (PE). The critical issue in relation to slowcrystallization rate of PLLA, resulting in poor heat resistance of end-use products, has attracted the great attention with such negative impact on PLLA manufacturing industries. Adding a nucleating agent in PLLA is an effective way to accelerate crystallization rate [12, 13]. As far as actual manufacturing is concerned, the usage of nucleating agent exhibits lower dosage, easer operation, crystallization enhancement effect, as well as excellent mechanical properties [14]. A variety of compounds such as inorganic salts [15, 16], organic small molecular compounds [1, 17], organic macromolecules [18-20] have been employed to accelerate PLLA's crystallization rate as nucleating agents. However, among these compounds, only a few can give rise to highly efficient PLLA crystallization accelerating ability, which are limited to talc [21], zinc phenylphosphonate [22], TMC series [23, 24], etc. For instance, it was reported that only 2 wt% talc caused half time of overall PLLA crystallization to be decreased by nearly 65 folds at 115°C [25].

It is vital to further improve PLLA's crystallization enhancing ability in order to meet stringent manufacturing requirements of end products. Since nucleation mechanism is still unclear for organic nucleating agents, more new organic nucleating agents are required to be further developed to identify common and critical groups used for PLLA crystallization. In this study, according to previous work [26] to evaluate positive effect of amide groups and benzene structures on PLLA crystallization, a new stearic hydrazide derivative, *N, N'*-bis(stearic acid)-1,4-dicarboxybenzene dihydrazide (PASH) was synthesized to investigate its influence on PLLA's crystallization and melting process, as well as thermal stability by means of differential scanning calorimetry (DSC) and thermogravimetric analysis (TGA). This study is conducive to broaden organic nucleating agent category, as well as confirms the important role of relevant molecular structures like amide group and benzene in enhancing PLLA crystallization.

2. Materials and methods

Materials and reagents

PLLA was produced by Nature Works LLC, USA, and it was purchased from Shenzhen Danshen Plastic Co., LTD. 1, 4-dicarboxybenzene, thionyl chloride, *N, N*-dimethylacetamide (DMF), stearic hydrazide and pyridine as reagents for synthesizing PSAH were supplied by Chongqing Chuandong Chemical Reagent Co., China without further modification.

PASH Synthesis

The synthetic route of PASH is given in Figure 1. First, 1, 4-dicarboxybenzene was added into 90 mL thionyl chloride with 3 mL DMF as a catalyst, the mixture was heated up to 85ºC *via* raising temperature by 5ºC to prevent violent boiling. Further, the mixture was held at 85ºC for 36h by continuous stirring. The resulting solution was evaporated by rotating in vacuum to prepare 1, 4-benzenedicarbonyl chloride.

Stearic hydrazide was dissolved in the mixed solution of 70 mL DMF and 3 mL pyridine, and subsequently 1, 4-benzenedicarbonyl chloride was slowly added into the aforementioned mixed solution, and the mixture was stirred at room temperature for 1.5 h, which was followed by stirring at 70ºC for 3 h. Such prepared mixed solution was poured into deionized water for the precipitation, and then filtration. The precipitation was further washed using deionized water 3 times. Finally, white PASH was dried in vacuum at 45ºC for 24 h. IR (KBr) υ: 3450.5, 3219.6, 3027.7, 2955.4, 2918.6, 2849.0, 1660.2, 1636.3, 1598.4, 1574.3, 1511.4, 1470.4, 1428.2, 1410.9, 1386.8, 1322.6, 1288.6, 1255.0, 1219.3, 1203.5, 1156.4, 1106.2, 1020.3, 970.3, 922.9, 877.2, 859.4, 807.4, 719.7, 649.9 cm^{-1}. And the characteristic absorption peaks are following: the absorption peak at 3450.5 cm^{-1} belongS to the stretching vibrations absorption of N-H, the peaks at 2918.6 cm^{-1} and 2849.0 cm^{-1} contribute to the antisymmetric stretching vibration and symmetric stretching vibration of C-H, the absorption peak at 1660.2 cm^{-1} belongs to the stretching vibration absorption of C=O of synthesized amide, the stretching vibration absorption of C=O of stearic hydrazide is at 1636.3 cm^{-1}, the vibration absorption peaks at 1598.4 cm^{-1}, 1574.3 cm^{-1} and 1511.4 cm^{-1} confirm the existence of benzene, the bending vibration absorption of C-N-H is at 1470.4

cm^{-1}, the absorption peaks at 877.2 cm^{-1} and 807.4 cm^{-1} contribute to out-of-plane bending vibration absorption of C-H, and 719.7 cm^{-1} contribute to the rocking vibration of CH_2. ^1H NMR (DMSO, 400 MHz) δ: 10.39 (s, 1H, NH), 9.82 (s, 1H, NH), 7.84～8.04 (m, 2H, Ar), 2.80～2.87 (m, 2H, CH_2), 2.16～2.19 (t, 4H, CH_2), 2.09～2.12 (t, 2H, CH_2), 1.67～1.70 (t, 2H, CH_2), 1.49～1.55 (t, 4H, CH_2), 1.24 (s, 2H, CH_2), 0.85～0.87 (t, 3H, CH_3).

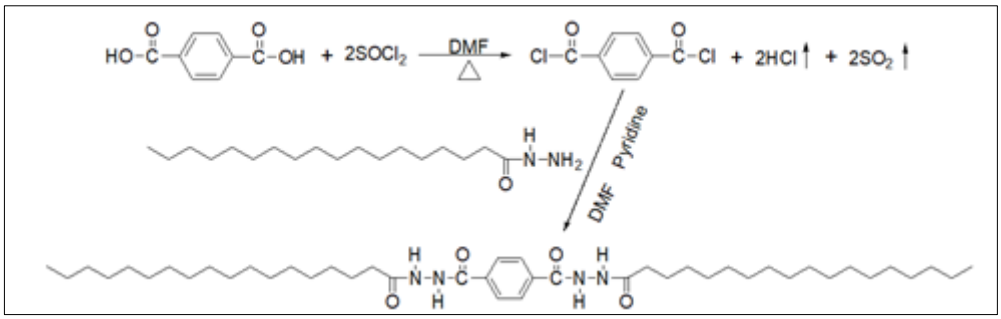

Figure 1. Synthetic route of PASH

PLLA/PASH preparation

PLLA/PASH was prepared using popular melt blending technology at different PASH concentration of 0.5, 1, 2 and 3 wt%. PLLA and PASH were dried under vacuum thoroughly for 24 h at 35ºC in order to remove thoroughly residual water. Melt blending took place at 190ºC with a rotor speed of 32 rpm for 7 min at the initial processing stage, and further at 32 rpm for 7 min at the second stage. The resulting blends were compressed into sheets with thickness of 0.4 mm using a hot press at 180ºC with the pressure of 20 MPa for 5 min, which was followed by cool press at room temperature under the same pressure level and duration.

Characterization methods

PASH Molecular structure characterization

The PASH's molecular structure was determined by IS50 Infrared Spectra in a wavenumber range from 4000 to 400 cm^{-1} and AVANCE 400MHz ^1H Nuclear Magnetic Resonance using dimethyl sulfoxide as a deuterium-substituted solvent.

Crystallization behavior

For pure PLLA and PLLA/PASH, the melt-crystallization and cold-crystallization were tested using Q2000 DSC apparatus under nitrogen at a rate of 50 mL/min. The temperature and heat flow were calibrated using an indium standard prior to DSC test. For the melt-crystallization process, the sample was firstly heated to 190ºC for 3 min to eliminate thermal history, and then cooled to 40ºC at different rates (1ºC/min, 2ºC/min and 5ºC/min). For the cold-crystallization process, the sample was cooled from the melt to 40ºC for 3 min, and the sample was heated to 190ºC at a rate of 1ºC/min.

The transmitted light intensity often increased with the increasing of crystallinity, thus, isothermal crystallization testes were carried out on a GJY-Ⅲ optical depolarizer in the temperature range from 105ºC to 125ºC, and the electronic signals transformed from optical depolarizer were amplified and recorded, finally the half time of overall crystallization $t_{1/2}$ was determined through further analysis.

Melting behavior

For melting behavior of PLLA/PASH after melt-crystallization at 1ºC/min, the melting process was recorded by Q2000 DSC apparatus, and the heating rate was set at 3ºC/min and 5ºC/min, respectively. The melting processes after isothermal crystallization at different crystallization temperatures (100ºC and 130ºC) for different time (60 min, 120 min and 180 min) were also recorded by Q2000 DSC apparatus, and the heating rate at melt stage was 10ºC/min.

Thermal stability

The thermal decomposition process of pure PLLA and PLLA/PASH was performed on a Q500 TGA device under air at a flow rate of 60 mL/min. The heating rate was controlled at 5°C/min in the temperature range from 35°C to 650°C.

3.Results and discussions

Non-isothermal crystallization

The melt-crystallization process of the modified semi-crystallization polyester can dramatically reflect the role of additives. As such, a comparative study on the melt-crystallization behavior of pure PLLA and PLLA/PASH was firstly performed. Figure 2 demonstrates the melt-crystallization DSC thermograms of pure PLLA and PLLA/PASH at 190°C with a cooling rate of 1°C/min. The melt-crystallization DSC thermograms of pure PLLA is clearly indicative of no melt-crystallization peak detected in pure PLLA. This finding suggests that pure PLLA's crystallization cannot occur in the cooling stage, which confirms its poor crystallization capability, as evidenced by previous studies [27, 28]. When compared with pure PLLA, PLLA/PASH apparently possesses sharp melt-crystallization peaks irrespective of different PASH concentrations, which proves that PASH exhibits an excellent hererogeneous nucleating effect for the purpose of enhancing PLLA crystallization. In view of molecular structure of PASH, intermolecular interactions during melt blending are easily formed owing to N-H of PASH as well as C=O of PLLA. Such interactions can induce molecular segments of PLLA to adjoin on the PASH surfaces as soon as possible, further resulting in accelerating PLLA's crystallization rate. As such, it is believed that amide group plays an important role in accelerating PLLA's crystallization rate to a certain degree. In addition, Figure 2 depicts the influence of PASH concentration on melt-crystallization process of PLLA. With increasing PASH concentration from 0.5 wt% to 3 wt%, it has been found that the melt-crystallization peak shifts towards lower temperature levels. In particular, the crystallization temperature decreases from 129.5 to 125.1°C. Although sufficient amount of PASH can offer more nucleation sites with much higher nucleation density, an excessive amount of PASH may increasingly imped the mobility of PLLA molecular segments, and further reduce PLLA's crystal growth rate. In this case the impact of PASH concentration can be highly detrimental to PLLA crystallization behavior, as earlier mentioned in our DSC results. Overall, PLLA/3% PASH yields the largest melt-crystallization enthalpy of 43.3 J/g as opposed to the sharpest melt-crystallization peak of PLLA/1% PASH. These results mentioned above evidently confirm the effective use of PASH as a heterogeneous nucleating agent can drastically accelerate PLLA crystallization.

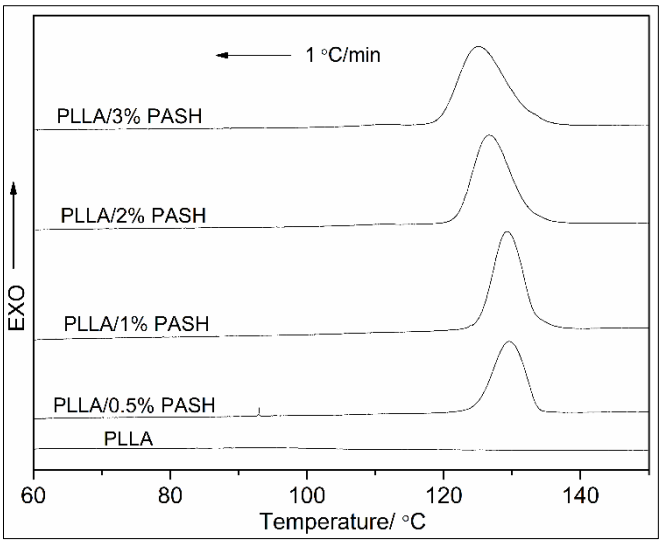

Figure 2. DSC melt-crystallization thermograms of pure PLLA and PLLA/PASH

In general, increasing cooling rate inevitably weakens the ability of nucleating agents for enhancing PLLA's crystallization [29]. Consequently, it is necessary to evaluate such a nucleating ability of additives on crystallization behavior of PLLA at a much higher cooling rate. Figure 3 depicts DSC melt-crystallization thermograms of PLLA/PASH at two different cooling rates of 2 and 5°C/min, respectively. It is clearly shown that melt-crystallization peak shifts towards lower temperature levels and becomes much wider when increasing cooling rate from 2 to 5°C/min. In particular, the melt-crystallization peak temperature of PLLA/2% PASH is even lower than 100°C at 5°C/min owing to the seriously negative effect of increasing cooling rate on nucleation ability of a nucleating agent again. Even then, all PLLA/PASH materials still possess distinct melt-crystallization peaks in DSC thermograms indicating significant nucleation ability of PASH within PLLA again.

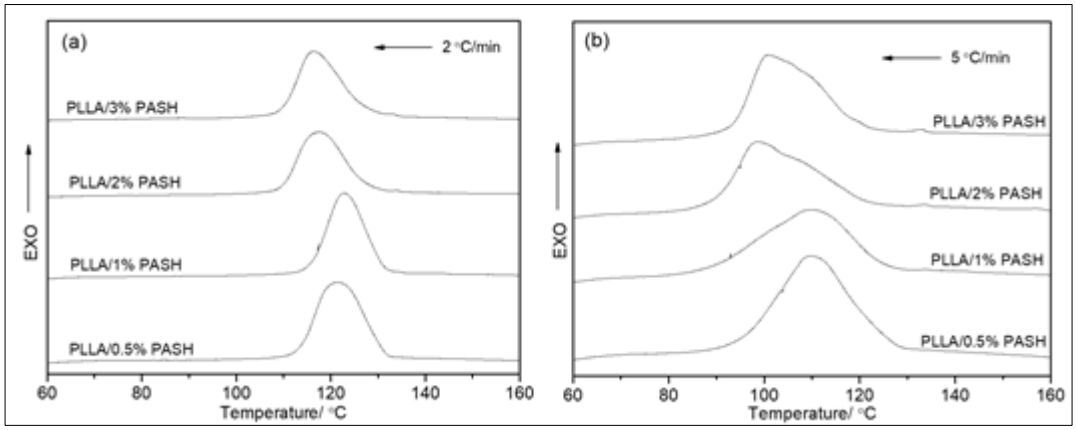

Figure 3. Melt-crystallization DSC thermograms of PLLA/PASH at different cooling rates: (a) 2 °C/min and (b) 5 °C/min

In the low temperature range, polymer itself often has a fast nucleation rate thanks to the overlap of molecular segments. As such, the investigation on the cold-crystallization process of PLLA/PASH is conducive to better understand the functionality of PASH in PLLA. As shown in Figure 4 with a heating rate of 1°C/min, the cold-crystallization peak has been detected to shift to lower temperature levels with increasing PASH loading, which can be attributed to increasing nucleation density of PASH with large amounts within PLLA. PASH and PLLA reveal heterogeneous and homogeneous nucleation effects, respectively and higher nucleation density can induce earlier crystallization. Nonetheless, apart from PLLA/3%PASH, subsequent melting peak of other PLLA/PASH turns to a slight shift toward higher temperatures when increasing PASH concentration in PLLA with the melting temperatures ranging from 150-175°C. This phenomenon implies imperfect crystal formation taking place in cold-crystallization processes since the existence of higher nucleation density gives rise to influence on their neighboring crystals during their growth.

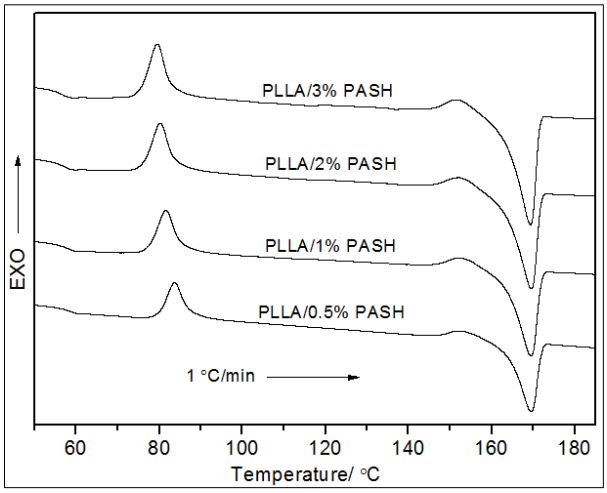

Figure 4. DSC thermograms for cold-crystallization process of PLLA/PASH at the heating rate of 1°C/min

Isothermal crystallization

Isothermal crystallization behaviors of pure PLLA and PLLA/PASH were further studied using a depolarized-light intensity technique. By recording the liner relationship between transmitted light intensity and crystallinity, $t_{1/2}$ was obtained at a given crystallization temperature, as illustrated in Figure 5 to plot $t_{1/2}$ as a function of crystallization temperature (T_c) for pure PLLA and PLLA/PASH at different PASH concentrations. With respect to pure PLLA, there is a slightly increasing tendency of $t_{1/2}$, which is followed by a decrease with the minimum $t_{1/2}$ value reaching 139.3 s at 120°C. Finally, $t_{1/2}$ increases again when the T_c is 125°C. Such an erratic alteration depends on a complex competitive relationship between the active ability and nucleation capability of macromolecular segments along with the variation of crystallization temperatures. The $t_{1/2}$ for PLLA/PASH with the T_c appears to be still irregular. However, it is evidently seen that $t_{1/2}$ decreases with increasing PASH loading in PLLA. In particular, PLLA/3%PASH has the minimum $t_{1/2}$ of 67.3 s at 105°C, and $t_{1/2}$ of pure PLLA is 310.1 s at corresponding T_c. The smaller $t_{1/2}$ of PLLA/PASH at a given T_c, in comparison to that of pure PLLA, confirms that PASH is able to enhance PLLA's crystallization rate.

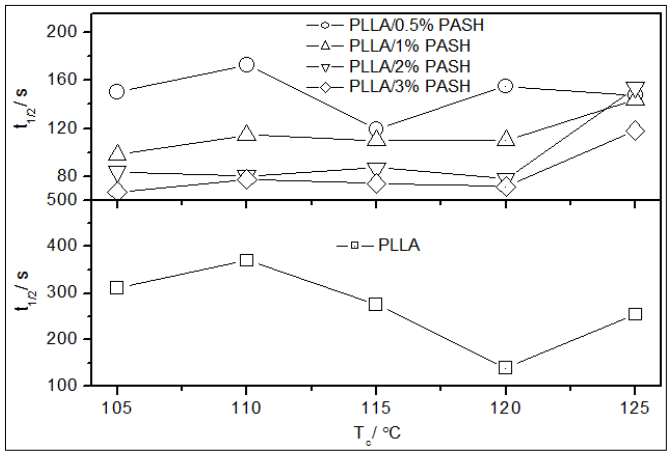

Figure 5. $t_{1/2}$ of pure PLLA and PLLA/PASH at different crystallization temperatures

Melting behavior

Thermal properties of semi-crystalline polyester also lies in the melting behavior because the crystallinity and perfection of crystal can directly affect subsequent melting process. Figure 6

demonstrates the melting behavior of PLLA/PASH after isothermal crystallization at two different temperatures (100 and 130°C) for different time. It can be found that there are existing double-melting peaks after isothermal crystallization at 100°C. According to melt-recrystallization mechanism [30], the low-temperature melting peak results from the melt of primary crystallites generated at 100°C. Whereas, the high-temperature melting peak is attributed to the melt of recrystallization during heating scan. As observed in Figure 6, there are very weak low-temperature melting peaks for all PLLA/PASH, which suggests that only a few crystals have been formed after crystallization at 100°C. Such a finding is associated with relatively low mobility of PLLA molecular segments at 100°C owing to very slow crystal growth. Moreover, the effect of crystallization time on melting temperature and shape of low-temperature melting peak and high-temperature melting peak seem to be negligible.

However, only single melting peak appears in DSC melting thermograms after crystallization at 130°C. The melting peak slightly shifts toward higher temperature level as increased crystallization time, resulting from more perfect PLLA crystals when increasing crystallization time in a high-temperature range, which is especially the case for PLLA/PASH with high mobility of molecular segments and higher nucleation rates.

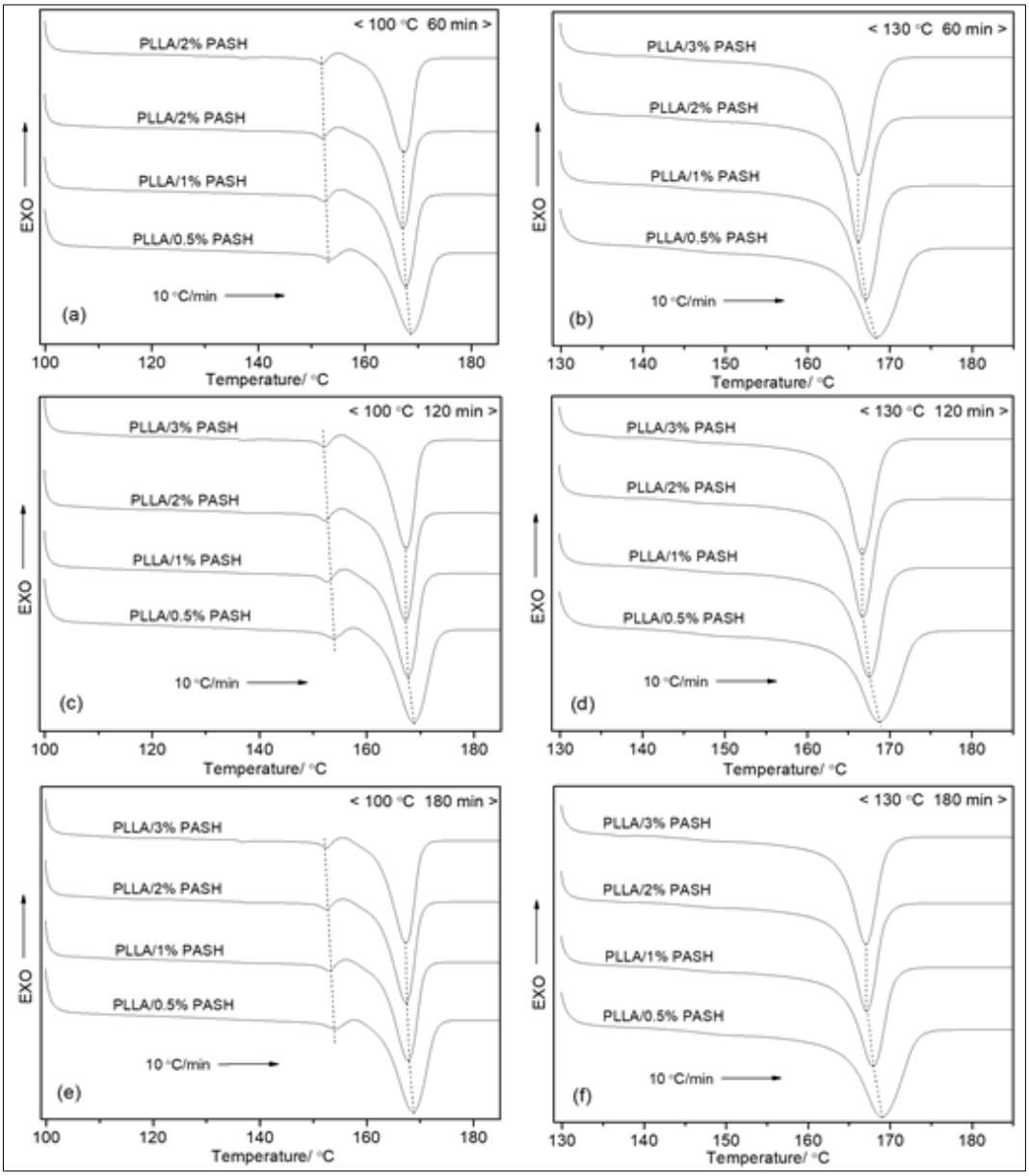

Figure 6. DSC thermograms for melting processes of PLLA/PASH after isothermal crystallization in different conditions: (a) 100°C and 60 min, (b) 130°C and 60 min, (c) 100°C and 120 min,

(d) 130°C and 120 min, (e) 100°C and 180 min and (f) 130°C and 180 min

The melting behavior of PLLA/PASH after non-isothermal crystallization was further evaluated through DSC analysis. Figure 7 depicts DSC melting thermograms of PLLA/PASH at different heating rates of 3 and 5ºC/min. When the heating rate is 3°C/min, any PLLA/PASH exhibits double-melting peaks, and the area ratio of low-temperature peak and high-temperature peak decreases as increased PASH loading. This phenomenon indicates that PLLA blended with a small amount of PASH is subjected to easy crystallization at the cooling stage, which is consistent with our DSC results for non-isothermal crystallization. On the other hand, a larger amount of PASH can provide more heterogeneous nucleation sites, enhancing the crystal growth at the heating stage. With increasing the heating rate from 3°C/min to 5°C/min, the high-temperature melting peak of PLLA containing a small amount of PASH gradually degenerates into a single peak with low-temperature melting peak because the higher heating rate can weaken the nucleation effect of PASH in heating, resulting in decreasing recrystallization in heating. However, PLLA still exhibits the double-melting peaks in DSC thermograms when PASH loading is beyond 1 wt% to generate recrystallization behavior.

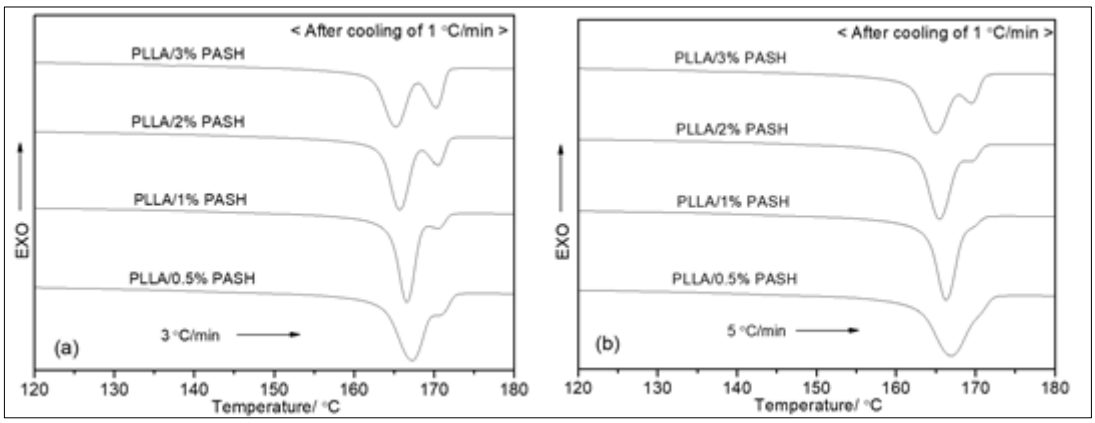

Figure 7. DSC thermograms of melting behavior of PLLA/PASH at different heating rates after non-isothermal crystallization: (a) 3°C/min and (b) 5°C/min

Thermal stability

The thermal stability of pure PLLA and PLLA/PASH under air from room temperature to 650 °C was evaluated using TGA instrument. As seen in Figure 8, all PLLA/PASH as well as pure PLLA have only one thermal weight loss stage in a temperature range of 275°C～375°C, which is often thought to be owning to the chain scissions and loss of ester groups [31, 32]. This result shows that PLLA's thermal decomposition profile does not depend on PASH at all in this study, which is related to very low dosage of PASH in PLLA and compatibility between PASH and PLLA to a certain degree [33]. Unfortunately, adding PASH significantly affects PLLA's onset thermal decomposition temperature (T_{od}). Overall, the incorporation of PASH decreases thermal stability. In particular, when PASH loading is between 0.5 and 2 wt%, T_{od} evidently decreases with increasing of PASH loading. However, the variation of T_{od} appears to be minor. Such a finding is associated with two major factors. First, a large amount of PASH further decreases PLLA's T_{od}. Second, the existence of a large amount of PASH can lead to stronger interactions between PLLA and PASH, which should be firstly destroyed by PLLA decomposition. Additionally, it is noted that the maximum difference of T_{od} between pure PLLA and PLLA/3%PASH is 29.7°C, but the minimum T_{od} originated from PLLA/3%PASH is still beyond 300°C in order to meet the daily use requirements.

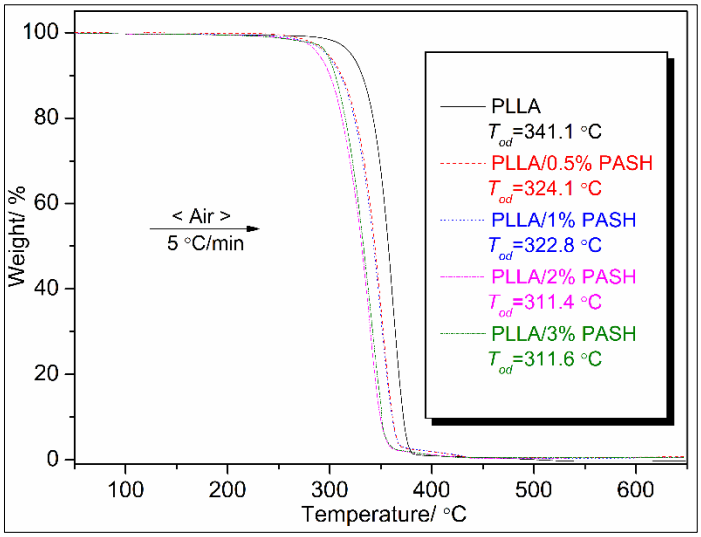

Figure 8. TGA thermograms of pure PLLA and PLLA/PASH

4.Conclusions

The thermal properties including melt-crystallization, cold-crystallization, isothermal crystallization, melting behavior and thermal stability of PLLA/PASH were studied in comparison with those of PLLA alone. The non-isothermal crystallization showed that PASH played an important role in enhancing crystallization ability by supplying heterogeneous nucleation sites in PLLA. With increasing PASH concentration, both melt-crystallization peak and cold-crystallization peak shifted toward lower temperature levels. However, the largest melt-crystallization enthalpy and the sharpest melt-crystallization peak were assigned to PLLA/3%PASH and PLLA/1%PASH, respectively. Additionally, for the melt-crystallization, an increase in cooling rate influenced negatively PLLA's crystallization. In isothermal crystallization from melting, all PLLA/PASH had the shorter $t_{1/2}$ than that of pure PLLA, and PLLA/3%PASH exhibited the minimum $t_{1/2}$ of 67.3 s at 105°C as opposed to $t_{1/2}$ of 310.1 s for pure PLLA. The crystallization temperature significantly affected melting processes of PLLA/PASH after isothermal crystallization. In particular, there were double-melting peaks after crystallization in a low temperature range. Whereas, only single melting peak appeared after crystallization in a high temperature range. Increasing heating rate undermined the crystallization in heating, resulting in high-temperature melting peak generated during the melting after non-isothermal crystallization. The addition of PASH was proven to dramatically decrease PLLA's thermal stability despite no change to thermal decomposition profile of PLLA induced by PASH.

Acknowledgements. This work was supported by Foundation of Chongqing Municipal Science and Technology Commission (cstc2017shmsA20021) and Scientific and Technological Research Program of Chongqing Municipal Education Commission (project number KJQN201801319).

References

1. FENG YQ, MA PM, XU PW, WANG RY, DONG WF, CHEN MQ, JOZIASSE C., The crystallization behavior of poly(lactic acid) with different types of nucleating agents [J], International Journal of Biological Macromolecules, 2018, 106: 955-962
2. KATHURIA A, BROUWERS N, BUNTINX M, HARDING T, AURAS R., Effect of MIL-53(Al) MOF particles on the chain mobility and crystallization of poly(L-lactic acid) [J], Journal of Applied Polymer Science, 2018, 135(3): 45690
3. LI Y, XIN SY, BIAN YJ, XU K, HAN CY, DONG LS., The physical properties of poly(L-lactide) and functionalized eggshell powder composites [J], International Journal of Biological Macromolecules, 2016, 85: 63-73

4. RADUSIN T, TOMSIK A, SARIC L, RISTIC I, BASCHETTI MG, MINELLI M, NOVAKOVIC A., Hybrid PLA/wild garlic antimicrobial composite films for food packaging application [J], Polymer Composites, 2019, 40(3): 893-900
5.AZNAR M, UBEDA S, DREOLIN N, NERIN C., Determination of non-volatile components of a biodegradable food packaging material based on polyester and polylactic acid (PLA) and its migration to food simulants [J], Journal of Chromatography A, 2019, 1583: 1-8
6. LI RJ, MA YL, ZHANG Y, ZHANG M, SUN DH., Potential of rhBMP-2 and dexamethasone-loaded Zein/PLLA scaffolds for enhanced in vitro osteogenesis of mesenchymal stem cells [J], Colloids and Surfaces-B-Biointerfaces, 2018, 169: 384-394.
7.SPINELLI G, LAMBERTI P, TUCCI V, IVANOVA R, TABAKOVA S, IVANOV E, KOTSILKOVA R, CIMMINO S, DI MAIO R, SILVESTRE C., Rheological and electrical behavior of nanocarbon/poly(lactic) acid for 3D printing application [J], Composites Part B-Engineering, 2019, 167: 467-476
8. YAO TY, DENG ZC, ZHANG K, LI SM., A method to predict the ultimate tensile strength of 3D pringting polylactic acid (PLA) materials with different printing orientations [J], Composites Part B-Engineering, 2019, 163: 393-402
9. ZHANG HX, BAI HW, DENG SH, LIU ZW, ZHANG Q, FU Q., Achieving all-polylactide fibers with significantly enhanced heat resistance and tensile strength via in situ formation of nanofibrilized stereocomplex polylactide [J], Polymer, 2019, 166: 13-20
10. KHARAZI AZ, FATHI MH, BAHMANI F, FANIAN H., Nonmetallic textile composite bone plate with desired mechanical properties [J], Journal of Composite Materials, 2012, 46(21): 2753-2761
11. LAI WY, FENG SW, CHAN YH, CHANG WJ, WWANG HT, HUANG HM., In vivo investigation into effectiveness of Fe_3O_4/PLLA nanofibers for bone tissue engineering applications [J], Polymers, 2018, 10(7): 804
12. FAN YQ, YU ZY, CAI YH, YAN SF, CHEN XS, YIN JB., Crystallization behavior and crystallite morphology controlling of poly(L-lactic acid) by adding *N*, *N'*-bis(benzoyl) sebacic acid dihydrazide [J], Polymer International, 2013, 62(4): 647-657
13.WEI ZY, SHAO SN, SUI ML, SONG P, HE MM, XU Q, LENG XF, WANG YS, LI Y., Development of zinc salts of amino acids as a new class of biocompatible nucleating agents for poly(L-lactide) [J], European Polymer Journal, 2019, 118: 337-346
14. XU XK, ZHEN WJ, BIAN SZ., Structure, performance and crystallization behavior of poly(lactic acid)/humic acid amide composites [J], Polymer-Plastics Technology and Engineering, 2018, 57(18): 1858-1872
15. DE ALMEIDA JFM, DA SILVA ALN, ESCOCIO VA, DA SILVA AHMDT, DE SOUSA AMF, NASCIMENTO CR, BERTOLINO LC., Rheological, mechanical and morphological behavior of polylactide/nano-sized calcium carbonate composites [J], Polymer Bulletin, 2016, 73(12): 3531-3545
16. WEI ZY, SHAO SN, SUI ML, SONG P, HE MM, XU Q, LENG XF, WANG YS, LI Y., Development of zinc salts of amino acids as a new class of biocompatible nucleating agents for poly(L-lactide) [J], European Polymer Journal, 2019, 118: 337-346
17. ZHENG HM, MA M, ZHENG QQ, ZHOU CW, CHEN S, WANG X., Effect of acylamino nucleating agent on crystallization behavior of poly(L-lactic acid) [J], Journal of Materials Science & Engineering, 2016, 34(6): 941-946
18. CAI J, LIU M, WANG L, YAO KH, LI S, XIONG HG., Isothermal crystallization kinetics of thermoplastic starch/poly(lactic acid) composites [J], Carbohydrate Polymers, 2011, 86(2): 941-947
19. YEH JT, YANG MC, WU CJ, WU X, WU CS., Study on the crystallization kinetic and characterization of poly(lactic acid) and poly(vinyl alcohol) blends [J], Polymer-Plastics Technology and Engineering, 2008, 47(12): 1289-1296
20. GUPTA A, SIMMONS W, SCHUEMEMAN GT, MINTZ EA., Lignin-coated cellulose nanocrystals as promising nucleating agent for poly(lactic acid) [J], Journal of Thermal Analysis and Calorimetry, 2016, 126(3): 1243-1251

21. CIPRIANO TF, DA SILVA ALN, DA SILVA AHMDFT, DE SOUSA AMF, DA SILVA GM, ROCHA MG., Thermal, rheological and morphological properties of poly(lactic acid)(PLA) and talc composities [J], Polimeros-Ciencia E Tecnologia, 2014, 24(3): 276-282
22. PAN PJ, LIANG ZC, CAO AM, INOUE Y., Layered metal phosphonate reinforced poly(L-lactide) composites with a highly enhanced crystallization rate [J], ACS Applied Materials & Interfaces, 2009,1(2): 402-411
23. ZHANG XQ, MENG LY, LI G, LIANG NM, ZHANG J, ZHU ZG, WANG R., Effect of nucleating agents on the crystallization behavior and heat resistance of poly(L-lactide) [J], Journal of Applied Polymer Science, 2016, 133(8): 42999
24. BAI HW, HUANG CM, XIU H, ZHANG Q, FU Q., Enhancing mechanical performance of polylactide by tailoring crystal morphology and lamellae orientation with the aid of nucleating agent [J], Polymer, 2014, 55(26): 6924-6934
25. HARRIS AM, LEE EC., Improving mechanical performance of injection molded PLA by controlling crystallinity [J], Journal of Applied Polymer Science, 2008, 107(4): 2246-2255
26. CAI YH, TANG Y, ZHAO LS., Poly(L-lactic acid) with organic nucleating agent *N, N, N'*-tris(1H-benzotriazole) trimesinic acid acethydrazide: Crystallization and melting behavior[J], Journal of Applied Polymer Science, 2015, 132(32): 42402
27. TIAN LL, CAI YH., Nucleated poly(L-lactic acid) with *N, N'*-oxalyl bis(benzoic acid) dihydrazide [J], Materials Research Express, 2018, 5(4): 045311
28. YE HM, HOU K, ZHOU Q., Improve the thermal and mechanical properties of poly(L-lactide) by forming nanocomposites with pristine vermiculite [J], Chinese Journal of Polymer Science, 2016, 34 (1): 1-12
29. CAI YH, ZHAO LS., Investigating on the modification of *N, N'*-adipic bis(benzoic acid) dihydrazide on Poly (L-lactic acid) [J], Polymer Bulletin, 2019, 76(5): 2295-2310
30. YASUNIWA M, SATOU T., Multiple melting behavior of poly(butylene succinate). Ⅰ. Thermal analysis of melt-crystallized samples [J], Journal of Polymer Science: Part B: Polymer Physics, 2002, 40(21): 2411-2420
31. ZHAO LS, CAI YH, LIU HL., *N, N'*-sebacic *bis*(hydrocinnamic acid) dihydrazide: A crystallization accelerator for Poly(L-lactic acid) [J], E-Polymers, 2019, 19: 141-153
32. ELSAWY MA, SAAD GR, SAYED AM., Mechanical, thermal, and dielectric properties of poly(lactic acid)/chitosan nanocomposites [J], Polymer Engineering and Science, 2016, 56(9): 987-994
33. ZUO YF, GU JY, ZHANG YH, WU YQ., Effect of plasticizer types on the properties of starch/polylactic acid composites [J], Journal of Functional Materials. 2015, 46: 6044-6048 (In Chinese)

Manuscreipt received: 1.06.2021